Journal of Theoretical and Applied Information Technology

31st December 2023. Vol.101. No 24

ISSN: 1992-8645 www.jatit.org E-ISSN: 1817-3195

MODELING, CALCULATION AND ANALYSIS OF ROBOTIC STRUCTURE MADE OF COMPOSITE MATERIAL UNDER DYNAMIC IMPACT

KAMIL KHAYRNASOV

Moscow Aviation Institute (National Research University), Moscow, Russian Federation

E-mail: khayrnasov_mai@mail.ru

ABSTRACT

The paper develops methods for calculating and analyzing robotic systems: multi-step dynamic systems under dynamic loading. At present, stands are made of magnesium alloys, which have good specific strength characteristics, and composite materials with higher specific strength characteristics are not used in the manufacture of stands. Therefore, the issues of researching stands made of composite material are important and relevant. The paper gives dependencies for determining the given characteristics of a multilayer composite material. Modeling and approximation of the stand by finite elements is given. The stand model had a three-layer structure: the model received the characteristics of the filler, and the surface of the model had the characteristics of a five-layer composite material. A technique for approximating the bench elements: bearings, gear rims and gearboxes by a system of rod elements of the same stiffness is proposed. An algorithm and a program for determining the stiffness of these elements have been developed. A technique has been developed for arranging a base made of a composite material along the lines of maximum stresses to ensure maximum rigidity of the stand. A comparative analysis of a stress-strain stand made of a composite and magnesium material has been carried out. Research methods can be applied to a wide class of robotic systems.

Keywords: *Robotic Systems; Benches; Modelling; Finite Element Method; Composite Materials; Stress-Strain State; Dynamic Loading*

1. INTRODUCTION

The need of the study is that at present stands are made of magnesium alloys, and composite materials with higher specific strength characteristics are not used.

The task of the study is to conduct a comparative analysis of a stress-strain stand made of composite and magnesium material.

The purpose of this study is to develop a methodology for calculating a robotic structure: imitation stand made of a composite material and magnesium alloy under operational loads. The difference from previous reviews is in the application of the dynamics and strength criteria of the composite material.

The relevance of the study is in the widespread use of robotic systems, including multistage dynamic stands that simulate flight characteristics in laboratory conditions and allow saving significant funds when testing products.

The novelty of the study is in the uniqueness of the hardware-in-the-loop (HIL) simulation stands, in the development of algorithm and program for calculating the rigidity of bearing supports, gear rims and gearboxes to replace them with bar systems identical in rigidity in a finite element approximation, in the development of a technique for arranging the base of a multilayer composite material along the trajectories of maximum stresses to ensure maximum strength and rigidity of the structure and in the calculation and analysis of the stress-strain state of HIL simulation stand for dynamic operational impacts, made of a composite material and a magnesium alloy.

The multi-stage dynamic benches of semi-natural simulation considered in the work designed to simulate the flight characteristics of systems used in aviation technology, have all the attributes of robotic systems [1-5]: movable modules, gearboxes, gear rims, bearing supports and control

systems [6-9]. The stands carry out the movement of the tested products in all degrees of freedom of the Cartesian coordinate system. Therefore, the methods developed in the article are applicable to robotic systems for various purposes in the textile and aviation industries [10]. At the same time, multi-stage dynamic stands have a different configuration, depending on the aircraft systems under study.

At present, most calculations are carried out using the finite element method [11-15], a modern numerical calculation method that has become widespread due to the development of computer technology. The finite element method is a numerical calculation method designed to determine the bearing capacity of structures under static and dynamic loads. The essence of the method is in the approximation of the structure by finite elements: rod, plate and volumetric elements. As a result of the calculation, generalized displacements at the nodal points of the finite elements are determined. Knowing the displacements, it is possible to determine the deformations and stresses. The behavior of the material in the elastic region does not depend on the type of loading. If the approximation of the majority of structural elements of a rod, shell or solid type can be performed using modern programs for discrediting the structure with finite elements, to approximate such elements as bearings, gearboxes, gear rims and methods to obtain adequate real models that take into account rigidity and deformation characteristics of such elements are required.

In the present study, a simulation of a multi-degree dynamic stand was carried out. The bench was approximated by finite elements. A technique has been developed for approximating bearing supports, gear rims and gearboxes, corresponding to their real response, rigidity and deformability. The stand made of magnesium alloy and carbon fiber was calculated for dynamic loads, the stress-strain state of the structure under complex stress was analyzed. The methods developed in the work are applicable to robotic systems, which are widely used in assembly shops and hazardous industries, where the presence of service personnel is unsafe, and in military affairs for monitoring the area and explosives disposal.

For inertial systems, which include robotic systems, inertial characteristics are of great importance, as a rule, the lower they are, the more efficiently such systems work. The inertial characteristics are more dependent on the material from which such systems are made.

One of the most effective materials in terms of specific strength is a composite material, which is becoming more widespread [16, 17]. The main disadvantage of the composite material is the low modulus of elasticity, which affects the deformation characteristics. At the same time, a multilayer composite material makes it possible to vary the strength and deformation characteristics depending on the location of the composite base. Since the composite material has a high specific strength, the article considers a robotic system: a multi-degree dynamic stand made of a composite material.

A significant number of works have been devoted to the study of structures made of composite materials for static and dynamic loads. In the article [18], the dynamics of thin-walled structures made of composite material is studied under the action of various force factors and the progression of destruction of composite structures under extreme conditions. In [19], methods for studying composite structures under impact loads of low speed are presented; data from experimental studies of various authors are used to confirm the reliability of the obtained results. The work [20] considers a stand made of a composite material under dynamic loads. The article [21] investigates the problem of reducing the structural integrity of sandwich panels with a honeycomb core under low-speed impact loads. The problem is solved numerically by an improved finite element method. The results of calculations are compared with experimental data: the form of damage and the beginning of destruction. In [22], the influence of the arrangement of layers of a multilayer composite material on mechanical strength is studied. The article [23] presents the results of static and dynamic analysis of three-layer plates consisting of external carrier layers and filler between the carrier layers. In [24], the bearing capacity of composite structures under high-speed loading is studied. The analysis of the received results is carried out. Composite materials have different structures. In [25], a new multi-point model has been developed for modeling composites with short fibers, which is highly effective for designing and modeling new composites with short fibers. In [26], the results of experiments on studying samples with off-axis fibers are presented to study the influence shear on compressive fracture toughness of multilayer composites when fibers are twisted. As a result, it

was revealed that at an off-axis angle of more than 10°, the splitting of the fiber bundle increases, followed by a violation of the compression of the fibers inside these bundles. There is a work [27] on predicting the failure of bearings connected to a composite. Two new criteria are proposed for predicting bearing failure on mechanically bonded composite joints. These criteria allow evaluating the load-bearing capacity of hybrid laminates in aircraft structures. Article [28] conducted a study of the strength of patches of composite material in aircraft products for reuse under various types of loading. Methods have been obtained to predict the strength of repaired products. In [29], an increase in delamination in a composite material is predicted. The results of the study show that as the delamination zone expands, the load-bearing capacity of a structure made of composite materials decreases. The work [30] presents a strategy for avoiding 3D collisions in collaborative robots, which is experimentally verified and proves the effectiveness of the proposed method due to which the number of emergency stops is reduced. In [31] there is a new virtual experimental testing methodology that uses virtual microstructures to study the interfiber failure of unidirectional carbon fiber reinforced polymer composites. The work [32] studied the effect of fiber orientation of carbon fiber composite material on the mechanical properties under tensile loading and analyzed the dynamic response using finite element analysis in ANSYS. Layer thickness is: for carbon fiber and resin it was adopted as 0.5 mm, with fiber orientations of 0°, 30°, 45°, 70° and 90°. In the static analysis, tensile stresses were determined according to von Mises, and deformations were also determined: total and equivalent. The natural frequencies of oscillations were also determined. As a result, it was revealed that a composite material with a fiber orientation of 0° has greater strength and a lower natural frequency than with fiber orientations of 30°, 45°, 70° and 90°.

Works [33-36] are devoted to the criteria for the destruction of multilayer materials under various assumptions. Not enough attention is also paid to the issues of research of robotic systems made of composite materials in the literature, as well as to multistage stands.

Currently, multistage dynamic stands are not made of composite material, but magnesium alloys are used. Therefore, it is important to study how the performance of a stand made of composite material changes in comparison with traditional materials. The use of composite materials with high specific strength characteristics in comparison with homogeneous materials in robotics requires increased attention. Inertial characteristics have a great influence on the positioning accuracy of the stand and, as a result, on the performance. To simulate a semi-natural simulation stand, it is necessary to determine the characteristics of a multilayer composite material consisting of layers of different arrangements of the base: composite fibers. To do this, it is necessary to determine the relationship between stresses and strains for a multilayer composite material depending on the arrangement of the base layers in the layers of the multilayer composite material.

This work is necessary for the development of methods for calculating complex dynamic structures. Research in this area is mainly devoted to individual structural elements. There is practically no work on the comprehensive calculation of complex robotic structures that take into account the mutual influence of the component parts. The work makes an additional contribution to the development of methods for calculating complex structures, such as multi-degree dynamic stands, consists in the use of composite materials instead of magnesium alloys traditionally used in the manufacture of stands, developed methods for modeling three-layer structures, programs and algorithms that allow taking into account the stiffness of elements such as bearings, gearboxes and ring gears.

2. MATERIALS AND METHODS

As a method for solving the problem of determining the stress-strain state of a structure under dynamic loading, we use Lagrange equation, which is applicable to solving static and dynamic problems of solid mechanics of a deformable body [21-24].

$$\frac{\partial}{\partial t}\frac{\partial T}{\partial \dot{q}_k} + \frac{\partial U}{\partial q_k} = Q, \quad (1)$$

where T is the kinetic energy of deformation of the structure, U is the potential energy of deformation of the structure, q is the vector of generalized displacements, index k is the number of degrees of freedom, t is the time, and the dot above the letter is the differentiation with respect to time.

2.1 Stress-Strain Relations Equations

In the present study, the parameters of a multilayer composite [34, 35] are obtained using the method of reduced characteristics.

We consider a plane-stressed state of an orthotropic material with coordinate axes coinciding with the axes of orthotropy of the material, then the relation between stresses and strains can be represented as:

$$\{\sigma\} = [E]\{\varepsilon\}, \quad (2)$$

where

$$[E] = \begin{Bmatrix} Q_{11} & Q_{12} & 0 \\ Q_{21} & Q_{22} & 0 \\ 0 & 0 & Q_{66} \end{Bmatrix}, \quad (3)$$

$$\{\varepsilon\}^T = \{\varepsilon_s, \varepsilon_\theta, \varepsilon_{s\theta}\},$$
$$\{\sigma\}^T = \{\sigma_s, \sigma_\theta, \sigma_{s\theta}\}, \quad (4)$$

$$Q_{11} = E_s/(1 - v_{s\theta}v_{\theta s}),$$
$$Q_{12} = v_{s\theta}E_s/(1 - v_{s\theta}v_{\theta s}),$$
$$Q_{21} = v_{\theta s}E_s/(1 - v_{s\theta}v_{\theta s}), \quad (5)$$
$$Q_{22} = E_\theta/(1 - v_{s\theta}v_{\theta s}),$$
$$Q_{66} = G_{66}.$$

where $\{\varepsilon\}^T = \{\varepsilon_s, \varepsilon_\theta, \varepsilon_{s\theta}\}$ is the deformation vector, $\varepsilon_s, \varepsilon_\theta, \varepsilon_{s\theta}$ are the deformations in the direction of the axis s, θ, and in the plane $s\theta$, $\{\sigma\}^T = \{\sigma_s, \sigma_\theta, \sigma_{s\theta}\}$ is the stress vector in the corresponding directions and plane, E_s, E_θ, $v_{s\theta,}v_{\theta s}$ are the modulus of elasticity, Poisson coefficients, G_{66} is the shear modulus.

The stress-strain relation matrix, when the coordinate axes are rotated through the angle θ, is transformed into the following form:

$$[\bar{E}] = \begin{Bmatrix} \bar{Q}_{11} & \bar{Q}_{12} & \bar{Q}_{16} \\ \bar{Q}_{21} & \bar{Q}_{22} & \bar{Q}_{26} \\ \bar{Q}_{61} & \bar{Q}_{62} & \bar{Q}_{66} \end{Bmatrix}, \quad (6)$$

where

$$\bar{Q}_{11} = c^4Q_{11} - s^4Q_{22} + 2(Q_{12} + 2Q_{66})s^2c^2,$$
$$\bar{Q}_{12} = (Q_{11} + Q_{22} - 4Q_{66})s^2c^2 + (s^2+c^2)Q_{22},$$
$$\bar{Q}_{16} = (c^2Q_{11} - s^2Q_{12} + (Q_{12} + 2Q_{66})(s^2-c^2))sc,$$
$$\bar{Q}_{22} = s^4Q_{11} - c^4Q_{22} + 2(Q_{12} + 2Q_{66})s^2c^2, \quad (7)$$
$$\bar{Q}_{26} = (s^2Q_{11} - c^2Q_{12} - (Q_{12} + 2Q_{66})(s^2-c^2))sc,$$
$$\bar{Q}_{66} = (Q_{11} - 2Q_{12} + Q_{22})s^2c^2 + (s^2-c^2)Q_{66},$$
$$s = \sin\theta\,, c = \cos\theta.$$

For a layer located at a distance z from the median plane, the deformations have the following form:

$$\{\varepsilon\} = \{\varepsilon^o\} + z\{\chi^o\}, \quad (8)$$

where $\{\varepsilon^o\}$ are the midsurface deformations and $\{\chi^o\}$ are the curvature deformations of median surface.

Substituting these relations into equation (2), we obtain the following dependencies:

$$\{\sigma\} = [\bar{Q}]\{\varepsilon^o\} + z[\bar{Q}]\{\chi^o\}. \quad (9)$$

Stresses can be represented using normal forces N and bending moments M:

$$\{N\} = \int_{-h/2}^{h/2}\{\sigma\}dz, \{N\}^T = (N_s, N_\theta, N_{s\theta}),$$
$$\{M\} = \int_{-h/2}^{h/2}\{\sigma\}zdz, \{M\}^T = (M_s, M_\theta, M_{s\theta}), \quad (10)$$

Integrating expression (10), we obtain:

$$\begin{Bmatrix} N \\ M \end{Bmatrix} = [E]\begin{Bmatrix} \varepsilon^o \\ \chi^o \end{Bmatrix}, [E] = \begin{bmatrix} [A] & [B] \\ [B] & [D] \end{bmatrix}, \quad (11)$$

where

$$[A] = \begin{bmatrix} A_{11} & A_{12} & A_{16} \\ A_{21} & A_{22} & A_{26} \\ A_{61} & A_{62} & A_{66} \end{bmatrix}, [B] = \begin{bmatrix} B_{11} & B_{12} & B_{16} \\ B_{21} & B_{22} & B_{26} \\ B_{61} & B_{62} & B_{66} \end{bmatrix}, [D] = \begin{bmatrix} D_{11} & D_{12} & D_{16} \\ D_{21} & D_{22} & D_{26} \\ D_{61} & D_{62} & D_{66} \end{bmatrix}. \quad (12)$$

$$\{A_{ij}, B_{ij}, D_{ij}\} = \int_{-h/2}^{h/2} Q_{ij}(1, z, z^2)\, dz\,, (i, j = 1,2,3). \quad (13)$$

Integrating expression (13) at constant values of the layer parameters in a multilayer composite, we have the following:

$$\begin{aligned} A_{ij} &= \sum_{k=1}^{n} \overline{Q}_{ij}\left(h_k - h_{k-1}\right), i, j = 1,2,6, \\ B_{ij} &= \sum_{k=1}^{n} \overline{Q}_{ij}\left(h^2{}_k - h^2{}_{k-1}\right), i, j = 1,2,6, \\ D_{ij} &= \sum_{k=1}^{n} \overline{Q}_{ij}\left(h^3{}_k - h^3{}_{k-1}\right), i, j = 1,2,6, \end{aligned} \quad (14)$$

where A_{ij}, B_{ij}, D_{ij} are the membrane, the flexural membrane and the flexural stiffnesses.

The notation used in expression (14) is given in the Figure 1.

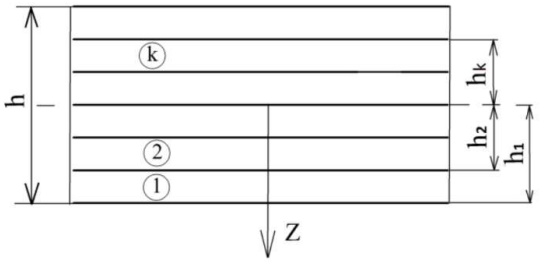

Figure 1. Multilayer structure of the composite material

2.2 Location of the Base in a Multilayer Composite Structure

To determine the location of the base in a multilayer composite, it is necessary to know the stress trajectories in order to locate the base along the lines of maximum stresses, ensuring maximum structural rigidity. In order to determine the lines of maximum stresses, in this work, a bench made of a homogeneous material was calculated for the action of static operational loads. Next, we determine the trajectories of maximum stresses and place the base of the bench material from a composite material along the lines of maximum stresses obtained from solving the problem of determining the stress-strain state of a bench made of a homogeneous material. In this case, it is necessary to place a certain number of layers at an angle to the lines of maximum stresses in order to perceive the shear stresses acting in the structure. The number of such layers is determined based on the analysis of the obtained results for sufficient safety margins from shear stresses (Figure 2).

2.3 Method for Determining the Rigidity of Gearboxes, Bearing Supports and Gear Rims

In this paper, the identification of such elements of robotic systems as bearings, gear rims and gearboxes are carried out in the finite element method by determining the rigidity characteristics of these elements and replacing them in the model with rod systems in terms of stiffness corresponding to the stiffness of the replaced bearings, gear rims and gearboxes. Since the direct modeling of these elements leads to an unjustified increase in the resolving equations and does not perform the functions of these elements in the model. The developed program for determining the stiffness of the elements under consideration takes into account the moments of inertia, angular accelerations and speeds, as well as gear ratios, stiffness and natural frequency of gearboxes and bearings. The Figure 3 shows the design diagram of a gearbox ratio designed to change the transmitted forces, speeds and accelerations. When calculating the reducer, it is necessary to calculate the equivalent diameter. The developed method and program for determining the stiffness and natural frequency of the gearbox makes it possible to calculate these characteristics for an arbitrary section of the gearbox shafts. The equivalent diameter allows determining the stiffness of the gearbox as a whole, the stiffness and the frequency.

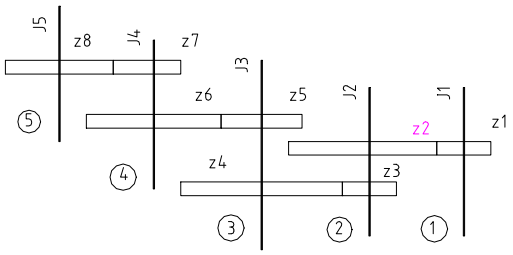

Figure 3. Calculation scheme of the pitch reducer

Initial data: moments of inertia of the shafts J_5,J_4,J_3,J_2,J_1 (kg×m×s^2), angular velocity υ_5 (1/s), angular acceleration ω_5 (1/s^2) and frequency f (Hz).

Gear ratios:

$$i_{54}=z_8/z_7\ i_{43}=z_6/z_5\ i_{32}=z_4/z_2\ i_{21}=z_2/z_1\ i_{11}=z_1/z_1. \quad (11)$$

Related to the input shaft, gear ratios:

$$i_{51}=i_{54}\times i_{43}\times i_{32}\times i_{21}\times i_{11},\ i_{41}=i_{51}/i_{54},\ i_{31}=i_{41}/i_{43},\ i_{21}=i_{31}/i_{32},\ i_{11}=i_{21}/i_{11}. \quad (16)$$

Gear ratio total:

$$i_{tot} = i_{54}\times i_{43}\times i_{32}\times i_{21}\times i_{11}. \quad (17)$$

Reduction gear ratio:

$$i_{red}= i_{43}\times i_{32}\times i_{21}\times i_{11}. \quad (18)$$

Moments of inertia reduced to the input shaft:

$$J_{51}=J_5/i_{51}^2,\ J_{41}=J_4/i_{41}^2,\ J_{31}=J_3/i_{31}^2,\ J_{21}=J_2/i_{21}^2,\ J_{11}=J_1/i_{11}^2. \quad (19)$$

Intermediate shaft acceleration:

$$\omega_4=\omega_5\times i_{54},\ \omega_3=\omega 4\times i43,\ \omega_2=\omega_3\times i_{32},\ \omega_1=\omega_2\times i_{21}. \quad (20)$$

$$M_5,\ M_4=J_4\times\omega_4+M_5/i_{54},\ M_3=J_3\times\omega_3+M_4/i_{43},\ M_2=J_2\times\omega_2+M_3/i_{32},\ M_1=J_1\times\omega_1+M_2/i_{21}. \quad (21)$$

Shaft load:

$$Pcircle=M_j/m\times z,\ Prad=Pcircle\times\tan 20^o, \quad (22)$$

where m is the module, z is the number of teeth and M_j is the moment on the shaft.

Support reactions R_1 and R_2 are determined by methods of resistance of materials, taking the moment of inertia of the shaft section $J_{shaft}=3.14\times D_{eq}^4/64$ based on D_{eq} (equivalent constant bending diameter).

Displacements and angles of rotation at the points of application of force and supports, respectively, are determined by the program.

Deformation of the Bearing from Fit on the Shaft and into the Body:

$$g_r=g_{r0}-\Delta d_1-\Delta D_2, \quad (23)$$

where g_{r0} is the ball bearing initial clearance, Δd_1 is the increase in the outer diameter of the inner ring from fit on the shaft and ΔD_2 is the decrease in the inner diameter of the outer ring from fit into the body are determined from the graphs [23] (p. 250), depending on the ratio of the stiffness of the mating parts:

- shaft (steel) $Cs=d_2/d$, bearing inner ring $Cinn=d/d_1$, bearing outer ring $Cout=D_2/D$, body (steel) $Cb=D/D_1$, where d_2 is the hollow shaft hole, d is the bearing inner ring inner diameter, d_1 is the outside diameter of bearing inner ring, D, D_2 are, respectively, the outer and inner diameter of the outer ring of the bearing and D_1 is the outer diameter of the body;
- ratios of deformations and fitting interferences in shaft-inner ring connections d_1/Hb and bodies with an outer ring D_2/Hk. $Hb=Hcp$ - H_1, Hav is the average value of the fit interference of the inner ring of the bearing, H_1 is the size of

irregularities, $H\kappa=Hav - H_1$ is also for bearing outer ring. D_1 is the increase in the outer diameter of the inner ring and D_2 is the reduction of inner ring outer diameter.

Bearing deformation under load:

$$\delta_r=\delta_{r1}+\delta_{r2}, \quad (24)$$

where δ_{r1} is the deformation in contact of the most loaded rolling element with the raceway in the bearing, and δ_{r2} is the radial compliance in contact of the bearing rings with the seating surfaces of the shaft and body.

Deformation in contact of the most loaded rolling element with the raceway in the bearing:

- with preload:

$$\delta_{r1}=\beta\times\delta_{r0}, \quad (25)$$

- with radial clearance:

$$\delta_{r1} = \beta \times \delta_{r0} - \frac{g_r}{2}. \quad (26)$$

The coefficient β taking into account the amount of preload or clearance in the bearing, is determined from the charts [23] (p. 211).

The value δ_{r0} for bearings of various types can be determined from the equations [23] (p. 208):

- for single-row ball:

$$\delta_{r0} = 2.0\times10^{-3} \times \sqrt[3]{\frac{Q_0^2}{D_T}}; \quad (27)$$

- for angular contact tapered bearing:

$$\delta_{r0} = 6.0 \times 10^{-4} \times \frac{Q_0^{0.9}}{\cos\alpha\times l^{0.8}}, \quad (28)$$

where R is the radial load on the support, i is the number of rows of rolling elements, z is the number of rolling elements in one row, $\alpha=arccos(1-g_r2\times A)$, α is the contact angle, D_T is the ball diameter, $d_{gr}=0.5232\times D_T$ groove diameter, $A=D_T\times(2\times d_{gr}D_T-1)$.

Radial compliance in contact of the bearing rings with the seating surfaces of the shaft and body:

$$\delta_{r2} = \frac{4\times R\times k}{\pi\times d\times B}\left(1+\frac{d}{D}\right), \quad (29)$$

where $k=0.015mm^2/kg$, D, d, B, respectively, are the outer, the inner diameters of the bearing and its width.

Calculation of gear rotation caused by elastic shaft deflection:

$$\varphi_{defl} = \frac{2}{m\times Z}\times\left(w_{circle} + w_{rad}\times tg20^o\right), \quad (30)$$

where w_{circle}, w_{rad} are the values of shaft deflections in the median plane of the transmission, respectively, in the circumferential and radial directions, taking into account deformations in the bearings, Z is the number of teeth, and m is the gear module.

Calculation of the error caused by the twisting of the shaft:

$$\varphi_{twist} = \sum(M\times l_i(G\times J_p), \text{ radian}, \quad (31)$$

where G is the shear modulus, $J_p=\pi\times(D^4-d^4)32$ is the polar moment of inertia, l_i is the length of the twisted section, and M is the moment on the shaft.

Calculation of the error caused by the compliance of the ring gear:

$$\varphi_{ring} = \frac{\mathrm{M}}{(k\times d^2\times b)}, \text{ radian}, \quad (32)$$

where d is the pitch diameter of the ring gear, b is the working width of the ring gear, and $k=368\ kg/mm^2$ is the experimental coefficient.

Calculation of error caused by keyed connection:

$$\varphi_{keyed\ con} = \frac{\mathrm{M}}{k_{keyed\ con}\times d_b^2\times l\times h\times z}, \text{ radian}, \quad (33)$$

where d_b is the shaft diameter, l is the key working length, h is the key height, z is the number of keys, $k_{keyed\ con}=15kg/mm^3$ for parallel keys, and $k_{keyed\ con}=25\ kg/mm^3$ for segment keys.

Error caused by the deformation of the pin connection:

$$\varphi_{pin}=k_{pin}\times M, \text{ radian}, \quad (34)$$

where k_{pin} is the proportionality factor [37] (p. 97). Total stiffness of the gearbox:

$$C = \left\{ \sum_{j=1}^{n} \left[\frac{(\phi_{defl} + \phi_{twist} + \phi_{ring} + \phi_{keyed\ con} + \phi_{pin})_j}{M_j \times i_j^2} \right] \right\}^{-1}, kg \times \text{т} \times rad, \quad (35)$$

where M is the moment on the shaft, φ is the angle of twist, i is the gear ratio related to the input shaft.

Reducer natural frequency:

$$f = \frac{1}{\pi} \times \sqrt{\frac{C \times i_{total}^2}{J_5}}, Hz, \quad (36)$$

where i_{total} is the total gear ratio, C is the rigidity, and J_5 is the reduced moment of inertia.

Calculated according to the developed program, rigidity of gearboxes, bearing supports and gear rims make it possible to replace these elements with a rod system identical in rigidity to the part under consideration. The results obtained were compared with the available experimental data, which confirmed the validity of such a replacement.

2.4 Modeling and Approximation

In the present study, modeling of a structure of complex geometry with surfaces of double curvature, moving elements and parts that ensure the movement of channels is carried out. A program has been developed for calculating the rigidity of gearboxes, bearing supports and gear rims. Approximation of the design model was carried out: multistage bench of semi-natural modeling with the identification of gearboxes, bearing supports and gear rims by a system of rod structures of identical rigidity. A technique has been developed for arranging the base of a multi-layer composite material along the trajectories of maximum stresses to ensure maximum rigidity, which is one of the main characteristics of the stand for precise positioning.

The bench model consists of a base connected to the yoke by a gear ring, a pitch ring fixed in the yoke bearings and a heel ring located inside the pitch ring and connected to the pitch ring by a gear. When modeling the bench, rod systems were used that imitate gearboxes, bearing supports and gear rims in terms of rigidity corresponding to these elements of the bench, plates, shell structures, three-layer shells in places of three-dimensional elements to increase the rigidity of the elements of the bench and three-dimensional elements. To approximate the stand with finite elements, solid 187 volume finite elements, shell 181 finite elements and contact finite elements were used.

The rigidity of the gearboxes was taken into account in the rigidity of the rod system.

We consider the procedure for modeling a stand of a three-layer structure made of a composite material:

- we model a three-degree HIL simulation bench in CATIA, assign the material characteristics to the structure given in the Table 4. This material serves as a light intermediate layer in a three-layer structure between the carrier layers, preventing the bearing layers from approaching and perceiving mainly shear stresses;
- next, we create surface elements for the entire structure, to which we further assign the characteristics of a multilayer composite package of five unidirectional layers with a given orientation: 0/45/0/-45/0 degrees;
- structural details that ensure the movement of the test bench channels (Figure 4), consisting of a system of rod elements identical in rigidity to the bearings in the connection of the heel channel and the pitch channel and the pitch channel and the forward fork, the toothed rim connecting the forward fork and the base, gearboxes in the place of transfer of forces to channels from the engines have the characteristics of the material made of steel and the characteristics of which are given in the Table 3.

The total number of finite elements of the partition was 310923. The total number of contact elements was 116804. The accuracy of the obtained calculations was checked by thickening the mesh of finite elements. The calculation error when partitioning into 184321 finite elements and the

adopted partitioning scheme was less than 3%. Rigid pinching of the stand base was used as the boundary conditions.

The Tables 1, 2, 3 and 4 show the characteristics of the materials used: magnesium alloy and carbon fiber [38-47].

The Figure 4 shows the finite element approximation of the stand model and the direction of the applied operational angular velocity of 500 deg/s.

2.5 Solution Method

To determine the stress-strain state and trajectories of maximum stresses for arranging the trajectories of the composite material base along them, when considering a bench made of a composite material, we consider a bench made of a homogeneous material under operational loads.

The solution of the problem is reduced to solving the system of linear algebraic equations.

$$[K]\{q\} = \{Q\}, \quad (37)$$

where $[K]$ is the stiffness matrix, $\{Q\}$ is the vector of external forces, and q is the generalized displacement.

In the future, we carry out the calculation of the bench made of composite material for the action of dynamic loading.

The equation for determining the complex stress-strain state of a bench made of composite material for dynamic effects is determined from the following equation:

$$[M]\{\ddot{q}\}+[K]\{q\} = \{Q\} - [N_{nl}], \quad (38)$$

where *[M]* is the mass matrix, $\{\ddot{q}\}$ are the generalized accelerations, the dot above the letter means differentiation with respect to time, and $[N_{nl}]$ are the nonlinear terms of the strain-displacement dependence calculated from the results of previous loading steps. At the first step, a linear problem is solved without a nonlinear term; at the second step, the nonlinear term is calculated from the generalized displacements calculated at the first loading step for the second and subsequent loading steps. To improve convergence, we can approximate the previous loading based on the results of approximating several previous loading steps using a parabolic or cubic dependence. When solving problems of dynamic loading of structures, it is necessary to set the minimum deviations of the model from the initial (equilibrium) state. To set the initial deviation of the model from the initial state, we can take the displacements obtained when solving the problem of the stress-strain state of the bench under static loading multiplied by 10^{-8}.

When solving problems of dynamic actions, special attention should be paid to the loading step and to reduce the loading step if the displacements of two subsequent loadings differ by more than 3-4%.

3. RESULTS AND DISCUSSION

The calculation of the stress-strain state of stands made of magnesium alloy (Figure 5) and a stand made of a three-layer material (Figure 6): with external bearing layers of a five-layer triaxial composite material (Table 3) and filler between the bearing layers of the material (Table 4).

Figure 6 shows a mosaic of stress isolines and the direction of the main stresses, allowing the trajectories of the base of the multilayer composite material to be positioned along the trajectories of maximum stresses, thereby ensuring maximum rigidity of the stand structure, which is one of the main factors affecting the accuracy of the stand positioning.

Figure 7 shows rod systems (colored in gold) that simulate bearings and a ring gear. In this case, the stiffness of the gearboxes was taken into account in the stiffness of the rod systems.

The Figure 8 shows the graphical data of a five-layer three-axis package: Young's moduli and shear in the polar coordinate system, thickness and orientation of the layers.

The Figure 9, 10 and 11 show the stress distribution mosaics in a five-layer three-axial composite material over layers with layer orientations of 0/45/0/-45/0 degrees, numbering of layers along the normal to the surface. The orientation axis of the layers is directed along the lines of maximum stresses and is equal to zero degrees.

In this study, the following criteria for the destruction of a composite material are considered: Tsai-Wu, Tsai-Hill and Hoffman [33-36].

The Figure 12 shows the most loaded sections of the bench structure. The most loaded layers of the composite material and the criteria for which failure can occur are given, indicating the layer of the composite material.

4. CONCLUSIONS

In conclusion, it should be noted that the problem being solved in the work, a comparative analysis of stress-strain stands made of magnesium and composite material, has been successfully solved. The purpose of the work is the development of methods for modeling, calculation and analysis of the bench for semi-natural simulation under dynamic loading. The reliability of the obtained results is confirmed by the convergence of the results of the finite element approximation of the stand and the reliability of ANSYS program, tested on a variety of examples and tasks. As a result of the study of stands made of magnesium alloy, traditionally used in the manufacture of a half-life simulation stand, and a stand made of carbon fiber, the stress-strain state of the stands was obtained under a dynamic inertial load from an angular operating speed of 500 deg/s. The analysis of the results of the stand made of magnesium alloy made it possible to arrange the composite material along the trajectories of maximum stresses and further correct the location of the base of the multilayer composite material along the lines of maximum stresses for the stand made of composite material. An analysis of the calculation results showed that the maximum stresses of the carbon fiber stand were 10% less than the maximum stresses calculated for the magnesium alloy stand with comparable displacements. The obtained layer-by-layer stresses of the composite material made it possible to apply the criteria for the destruction of a multilayer composite material and to identify the layer, direction and type of stress (tensile or compression) that destroys the multilayer composite material. Considering that carbon fiber has an allowable stress 1.3-1.6 times higher than that of magnesium alloy, the production of semi-natural simulation stands from composite materials is a promising direction since HIL simulation stands are robotic systems with bearings, gear rims, gearboxes and movable channels. The strength of the research is the developed methods for calculating and studying structures made of composite materials containing bearings, gearboxes and gears, which are inadequately implemented in computer-aided design systems. The reliability of the obtained results is confirmed by the use of ANSYS program, checked on a large number of test examples, and the convergence of the obtained results, verified by refinement of the finite element mesh. A weakness of the study is the paucity of available experimental studies.

The developed methods are applicable to a wide class of tasks of robotic systems made of homogeneous and composite materials under static and dynamic loads.

Directions for future research include the development of methods for the kinematic behavior of robotic systems, calculation and analysis of natural frequencies of oscillations.

ACKNOWLEDGEMENT

This work was supported financially by the Russian Science Foundation under the Scientific Project № 22-29-20299 (the recipient is K.Z. Khayrnasov, https://rscf.ru/project/22-29-20299/).

REFRENCES

[1]. Tian, Y.; Chen, C.; Sagoe-Crentsil, K.; Zhang, J.; Duan, W. Intelligent robotic systems for structural health monitoring: Applications and future trends. *Autom. in Constr.* 2022, *139*, 104273. https://doi.org/10.1016/j.autcon.2022.104273

[2]. Tao, B.; Feng, Y.; Fan, X.; Zhuang, M.; Chen, X.; Wang, F.; Wu, Y. Accuracy of dental implant surgery using dynamic navigation and robotic systems: An in vitro study. *J. of Dent.* 2022, *123*, 104170. https://doi.org/10.1016/j.jdent.2022.104170 robotic

[3]. Xu, X.; Chen, Y.; Zou, B.; Gong, Y. Assignment of parcels to loading stations in robotic sorting systems. Transportation *Res. Part E: Log. and Transp. Rev.* 2022, *164*, 102808. https://doi.org/10.1016/j.tre.2022.102808

[4]. Boschetti, G.; Faccio, M.; Granata, I.; Minto, R. 3D collision avoidance strategy and performance evaluation for human–robot collaborative systems. *Comp. & Industr. Eng.* 2023, *179*, 109225. https://doi.org/10.1016/j.cie.2023.109225

ISSN: 1992-8645 www.jatit.org E-ISSN: 1817-3195

[5]. Tawk, C.; Alici, G. Finite element modeling in the design process of 3D printed pneumatic soft actuators and sensors. *Robot.* 2020, *9(3)*, 52. https://doi.org/10.3390/robotics9030052

[6]. Lindqvist, B.; Karlsson, S.; Koval, A.; Tevetzidis, I.; Haluška, J.; Kanellakis, C.; Nikolakopoulos, G. Multimodality robotic systems: Integrated combined legged-aerial mobility for subterranean search-and-rescue. *Robot. and Autonom. Syst.* 2022, *154*, 104134. https://doi.org/10.1016/j.robot.2022.104134

[7]. Guo, Y.; Parker, R.G. Stiffness matrix calculation of rolling element bearings using a finite element/contact mechanics model. *Mechan. and Mach. Theory* 2012, *51*, 32-45. https://doi.org/10.1016/j.mechmachtheory.2011.12.006

[8]. Hoopert, I. Advanced analytical approach for calculating ball and roller bearings. *J. of Tribol.* 2014, *136*, 11105-11116.

[9]. Dewangan, P.; Parey, A.; Hammami, A.; Chaari, F.; Haddar, M. Dynamic characteristics of a wind turbine gearbox with amplitude modulation and gravity effect: Theoretical and experimental investigation. *Mechan. and Mach. Theory* 2022, *167*, 104468.

[10]. Liu, L.; Zhu, L.; Gou, X. Modeling and analysis of load distribution ratio and meshing stiffness for orthogonal spur-face gear drive under point contact. *Mechan. and Mach. Theory* 2023, *182*, 105239. https://doi.org/10.1016/j.mechmachtheory.2023.105312

[11]. Mitrofanov, O.V. Current problems and basic relationships for investigations of composite panels with asymmetric structure taking into account geometric nonlinearity. *Nat. and Eng. Sci.* 2021, *2*, 140-144.

[12]. Barbero, E.J. *Finite Element Analysis of Composite Materials using Abaqus®*; CRC press: Boca-Raton, USA, 2023.

[13]. Zienkiewicz, O.C.; Taylor, R.L.; Zhu, J.Z. *Finite element method: its basis and fundamental*; Butterworth-Heinemann: Oxford, UK, 2013.

[14]. Moaveni, S. *Finite Element Analysis Theory and Application with ANSYS*; Pearson Education: London, UK, 2015.

[15]. Koutromanos, I. *Fundamentals of finite element analysis: linear finite element analysis*; John Wiley & Sons: New York, UK, 2018)

[16]. Bathe, K.J. *Finite element procedures*; Pearson education Inc.: New York, UK, 2006.

[17]. Chawla, K.K. *Composite materials: science and engineering*; Springer Science & Business Media: New York, USA, 2012.

[18]. Daniel, I.; Werner, B.; Fenner, J.; Cho, J.M. Mechanical and failure behavior of composite materials under static and dynamic loading. In 50th AIAA/ASME/ASCE/AHS/ASC Structures, Structural Dynamics and Materials Conference, USA, 14 June 2009. https://doi.org/10.2514/6.2009-2425

[19]. Hinton, M.J.K.A.; Kaddour, A.S.; Soden, P.D. *Failure criteria in fibre reinforced polymer composites: the world-wide failure exercise*; Elsevier: Oxford, UK, 2004.

[20]. Werner, B. T., Schaefer, J. D., & Daniel, I. M. Deformation and failure of angle-ply composite laminates. In *Experimental Mechanics of Composite, Hybrid, and Multifunctional Materials, Volume 6: Proceedings of the 2013 Annual Conference on Experimental and Applied Mechanics*; Springer International Publishing: Cham, Switzerland, 2013.

[21]. Vasiliev, V.V.; Morozov, E.V. *Advanced mechanics of composite materials and structures*; Elsevier: Cambridge, UK, 2018.

[22]. Phadnis, V.A.; Silberschmidt, V.V. *8.14 Composites under dynamic loads at high velocities*; Elsevier: Cambridge, UK, 2018.

[23]. Kim, H.-G.; Wiebe, R. Numerical investigation of stress states in buckled laminated composite plates under dynamic loading. *Compos. Struct.* 2018, *235*, 111743. https://doi.org/10.1016/j.compstruct.2019.111743

[24]. Correas, A.C.; Ghasemnejad, H. Analytical development on impact behaviour of composite sandwich laminates by differentiated loading regimes. *Aerosp. Sci. and Techn.* 2022, 126, 107658. https://doi.org/10.1016/j.ast.2022.107658 1270-9638/

[25]. Cheung, H.L.; Mirkhalaf, M. A multi-fidelity data-driven model for highly accurate and computationally efficient modeling of short fiber composites. *Compos. Sci. and Techn.* 2024, 246, 110359. https://doi.org/10.1016/j.compscitech.2023.110359

[26]. He, R.; Cheng, L.; Gao, Y.; Cui, H.; Li, Y. The fibre kinking fracture toughness of laminated composites under combined compression and shear. *Compos. Sci. and Techn.* 2023, 244, 110307.

https://doi.org/10.1016/j.compscitech.2023.110307

[27]. Wallner, C.; Almeida, S.F. Fracture criteria and surrogate models for bearing strength of mechanically fastened joints on hybrid composite laminates. *J. of Compos. Mat.* 2023, 0(0), 00219983231215484. https://doi.org/10.1177/00219983231215484

[28]. Couto, R.F.M.; Couto, A.M.S.; Arachchige, D.D.S., Nascimento, D.R.; Moreira, R.D.F.; de Moura, M.F.S.F.; Vaz, M.P. Numerical analysis on the strength prediction of composite bonded repairs under different loading scenarios. *J. of Comp. Mat.* 2023, 00219983231179789.

[29]. Alizadeh, F.; Sebdani, R.M.; Soares, C.G. Numerical analysis of the residual ultimate strength of composite laminates under uniaxial compressive load. *Comp. Struct.* 2022, 300, 116161. https://doi.org/10.1016/j.compstruct.2022.116161

[30]. Boschetti, G.; Faccio, M.; Granata, I.; Minto, R. 3D collision avoidance strategy and performance evaluation for human–robot collaborative systems. *Comp. & Industr. Eng.* 2023, 179, 109225. https://doi.org/10.1016/j.cie.2023.109225

[31]. Zhang, B.; Ge, J.; Cheng, F.; Huang, J.; Liu, S.; Liang, J. Failure prediction for fiber reinforced polymer composites based on virtual experimental tests. *J. of Mat. Res. and Techn.* 2023, 24, 8924-8939. https://doi.org/10.1016/j.jmrt.2023.05.123

[32]. Noman, A.A.; Shohel, S.M.; Riyad, S.H.; Gupta, S.S. Investigate the mechanical strength of laminated composite carbon fiber with different fiber orientations by numerically using finite element analysis. In *Materials Today: Proceedings* 2023 https://doi.org/10.1016/j.matpr.2023.02.132

[33]. Latyshev, O.G.; Veremeychik, A.B.; Zhukov, E.A. *Application of composite materials in stands for dynamic loading*; Publishing house of MSTU N.E. Bauman: Moscow, Russia, 2011.

[34]. Manes, A.; Gilioli, A.; Sbarufatti, C.; Giglio, M. Experimental and numerical investigations of low velocity impact on sandwich panels. *Compos. Struct.* 2013, *99*, 8-18. https://doi.org/10.1016/j.compstruct.2012.11.031.

[35]. Noman, A.A.; Shohel, S.M.; Riyad, S.H.; Gupta, S.S. Investigate the mechanical strength of laminated composite carbon fiber with different fiber orientations by numerically using finite element analysis. *Mater. Tod.: Proceed.* 2023, preprint. https://doi.org/10.1016/j.matpr.2023.02.132

[36]. Lin, J.P.; Liu, X.; Wang, Y.; Xu, R.; Wang, G. Static and dynamic analysis of three-layered partial-interaction composite structures. *Eng. Struct.* 2022, *252*, 113581. https://doi.org/10.1016/j.engstruct.2021.113581

[37]. Zhang, B.; Ge, J.; Cheng, F.; Huang, J.; Liu, S.; Liang, J. Failure prediction for fiber reinforced polymer composites based on virtual experimental tests. *J. of Mat. Res. and Techn.* 2023, *24*, 8924-8939.

[38]. Daniel, I.M. Yield and failure criteria for composite materials under static and dynamic loading. *Progr. in Aerosp. Sci.* 2016, *81*, 18-25. https://doi.org/10.1016/j.paerosci.2015.11.003.

[39]. Gu, J.; Chen, P.; Su, L.; Li, K. A theoretical and experimental assessment of 3D macroscopic failure criteria for predicting pure inter-fiber fracture of transversely isotropic UD composites. *Comp. Struct.* 2021, *259*, 113466.

[40]. Sun, Q.; Zhou, G.; Meng, Z.; Guo, H.; Chen, Z.; Liu, H.; Kang, H.; Keten, S.; Su, X. Failure criteria of unidirectional carbon fiber reinforced polymer composites informed by a computational micromechanics model. *Comp. Sci. and Techn.* 2019, *172*, 81-95. https://doi.org/10.1016/j.compscitech.2019.01.012.

[41]. Davila, C.G.; Camanho, P.P.; Rose, C.A. Failure criteria for FRP laminates. *J. Compos. Mat.* 2005, *39(4)*, 323-345.

[42]. Childs, P.R. Rolling Element Bearings In *Mechanical Design*; Elsevier Ltd.: Oxford, UK, 2021

[43]. Beizelman, R.D.; Tsypkin, B.V.; Perel, L.Ya. *Rolling bearings*; Mashinostroenie: Moscow, USSR, 1975.

[44]. Dmitriev, F.S. *Design of gearboxes for precision instruments*; Mashinostroenie: Leningrad, USSR, 1971.

[45]. Gunyaev, G.M.; Zhigun, I.G.; Dushin, M.I.; Vorontsov, I.A.; Yakushin, V.A.; Rumyantsev, A.F. Dependence of elastic and strength characteristics of high-modulus composites on reinforcement schemes. *Polym. Mech.* 1974, *6*, 1019-1027.

[46]. Reinforcement of building structures with carbon tapes. Available online: usilenieyug.ru/stati/ (accessed on 10 April 2023).

ISSN: 1992-8645 www.jatit.org E-ISSN: 1817-3195
[47]. Operational materials: Carbon fiber. Available online: http://ustroistvo-avtomobilya.ru/e-kspluatatsionny-e-materialy/ugleplastiki/ Available online: usilenieyug.ru/stati/ (accessed on 10 April 2023).

Journal of Theoretical and Applied Information Technology
31st December 2023. Vol.101. No 24

ISSN: 1992-8645 www.jatit.org E-ISSN: 1817-3195

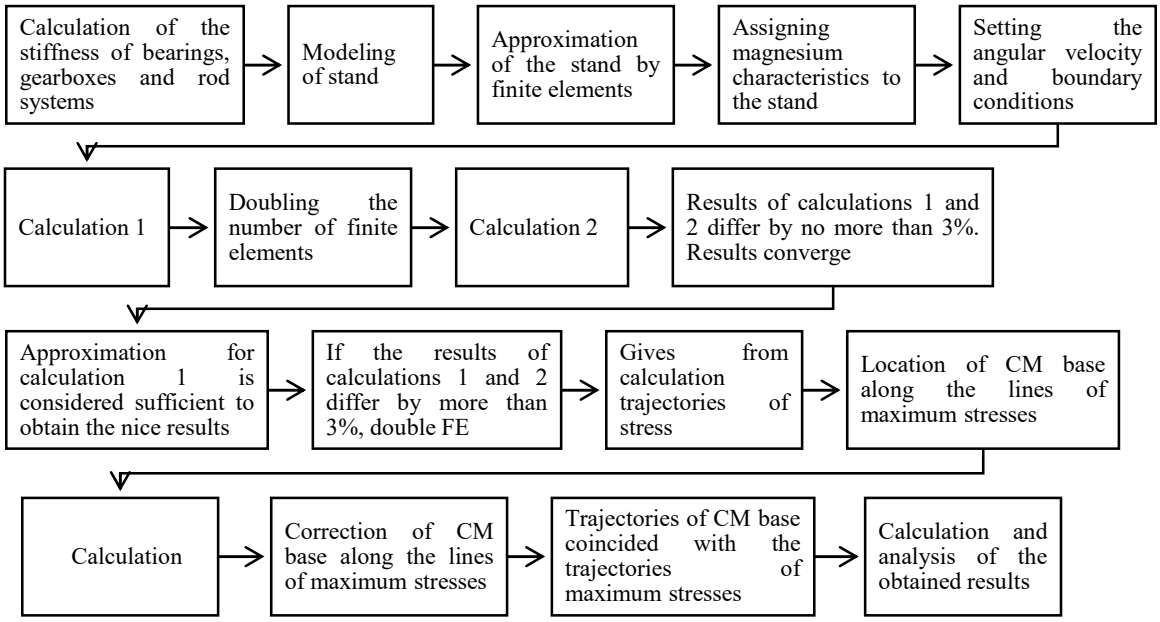

Figure 2. Flowchart of calculation (CM - composite material, FE - finite elements)

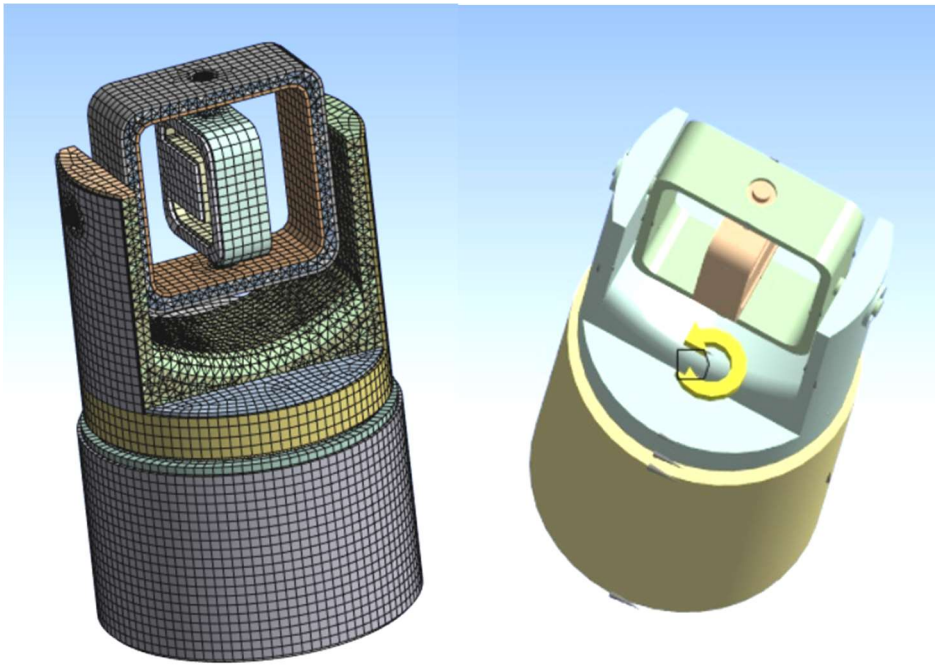

Figure 4. Finite element approximation of the stand model and the direction of the stand movement from the angular operating speed of 500 deg/s applied to the course fork

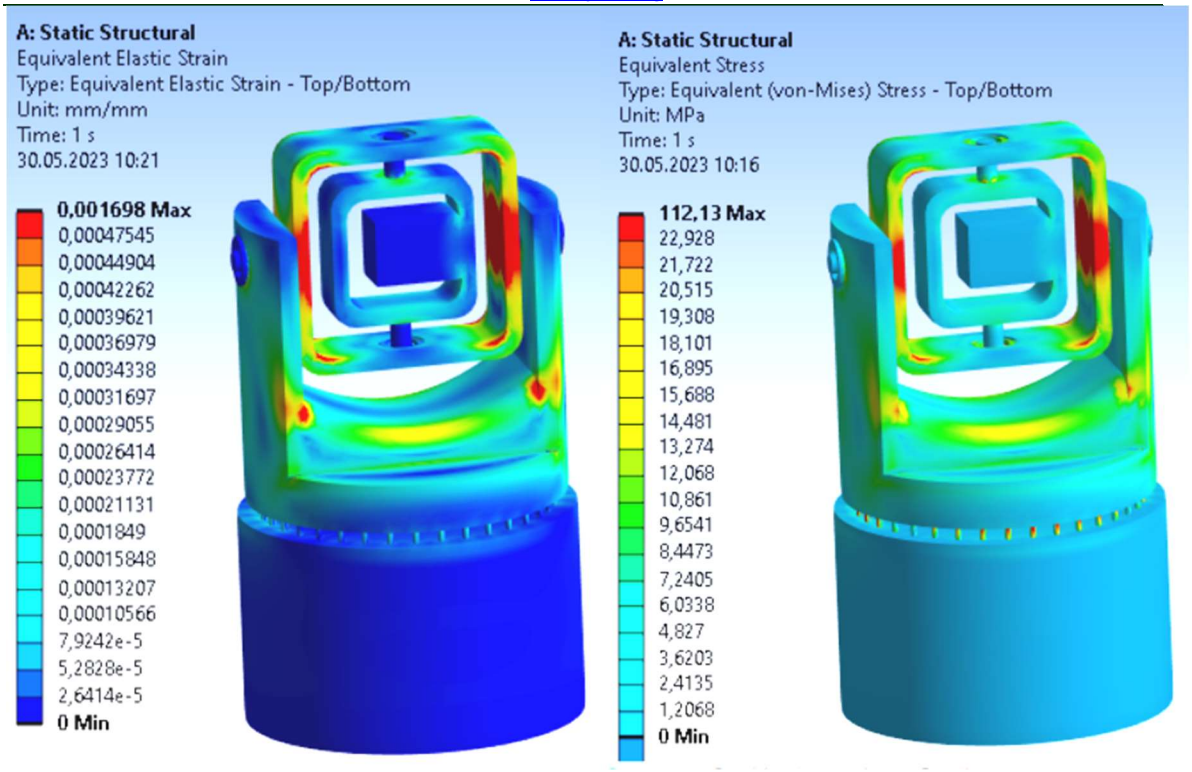

(**a**) (**b**)

Figure 5. Mosaic of (a) displacements and (b) stresses along the Mises of a carbon fiber stand under the action of an angular load of 500 deg / s applied to the course fork

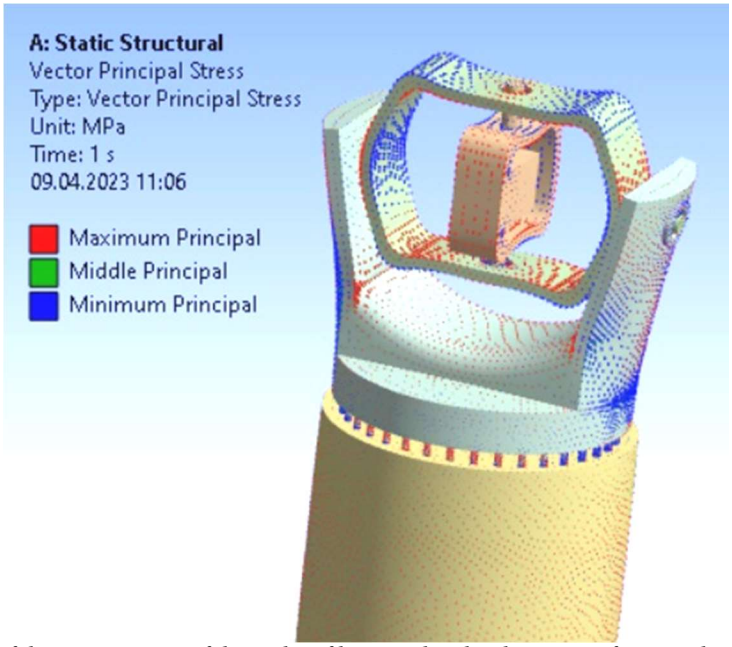

Figure 6. Direction of the main stresses of the carbon fiber stand under the action of an angular velocity of 500 deg/s applied to the course fork

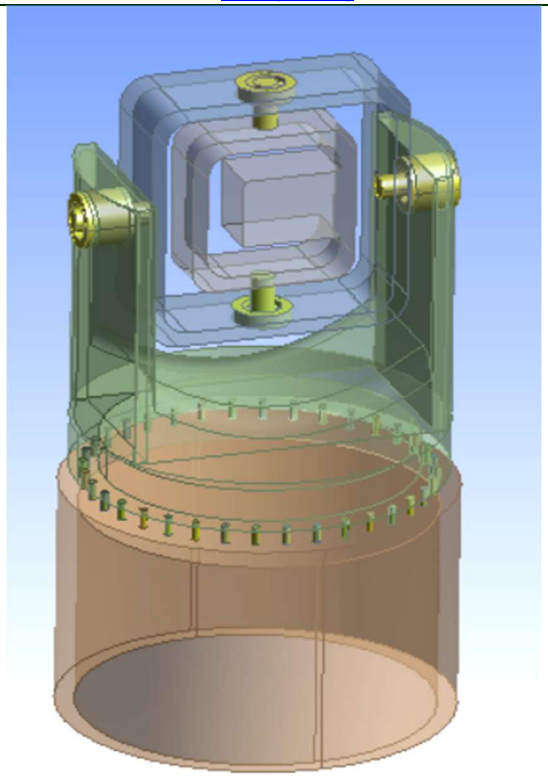

Figure 7. Approximation of bearings, ring gear in the stand by replacing them with rod systems of identical stiffness (painted in golden color)

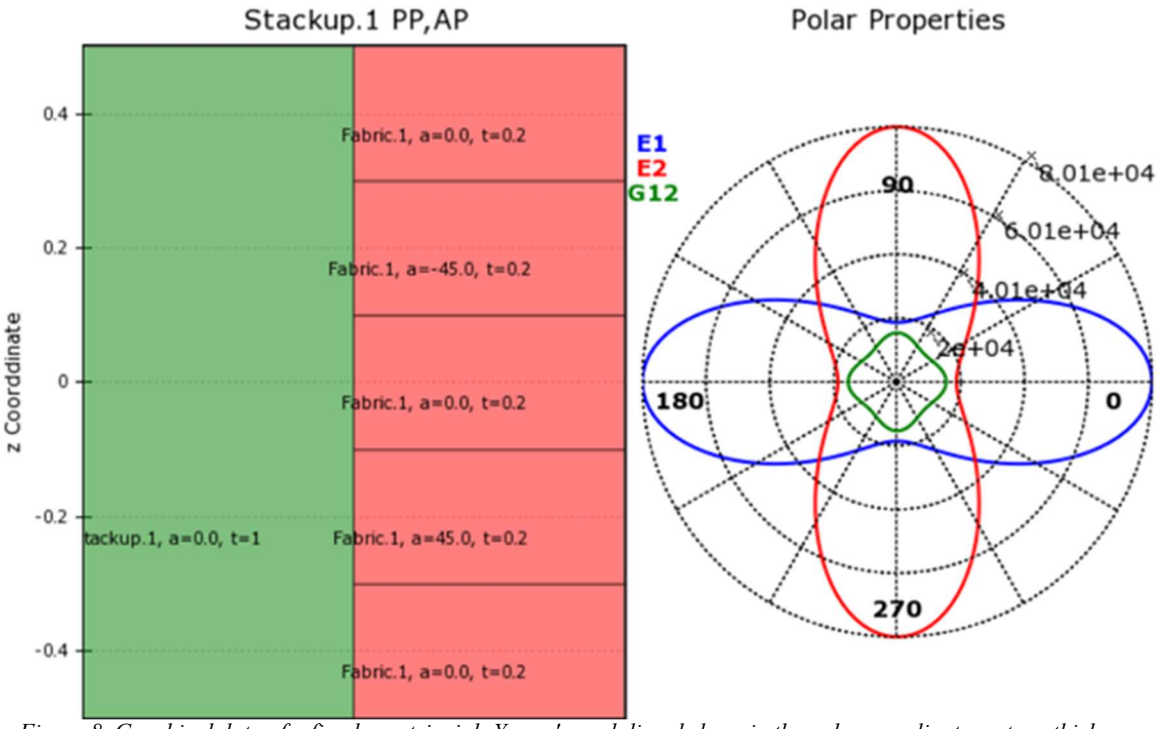

Figure 8. Graphical data of a five-layer triaxial: Young's moduli and shear in the polar coordinate system, thickness and orientation of the layers

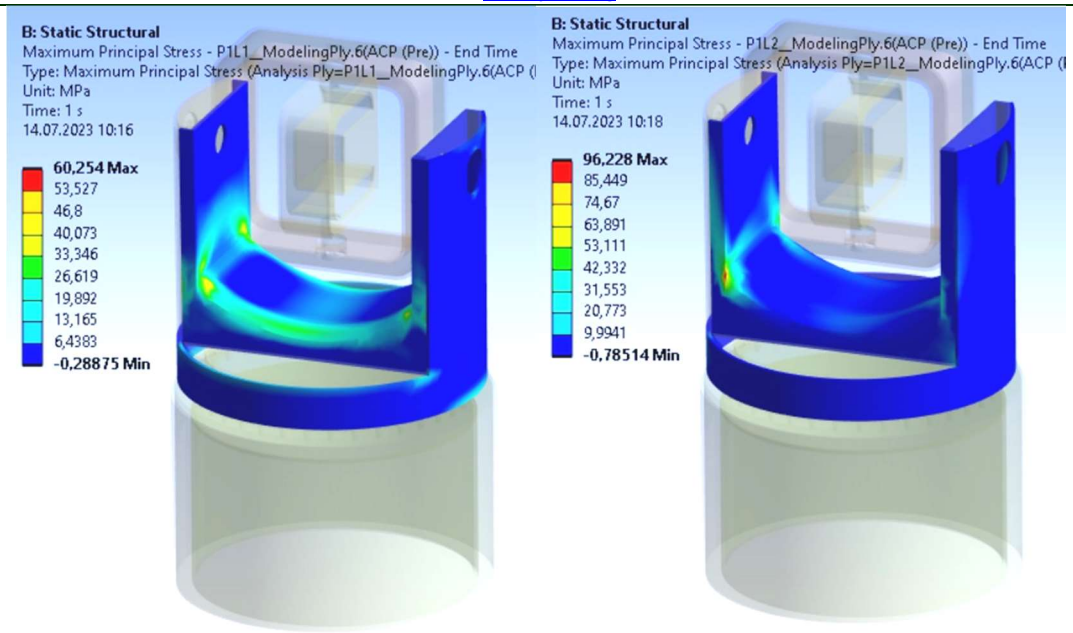

Figure 9. Stresses in the first and second layer of the composite

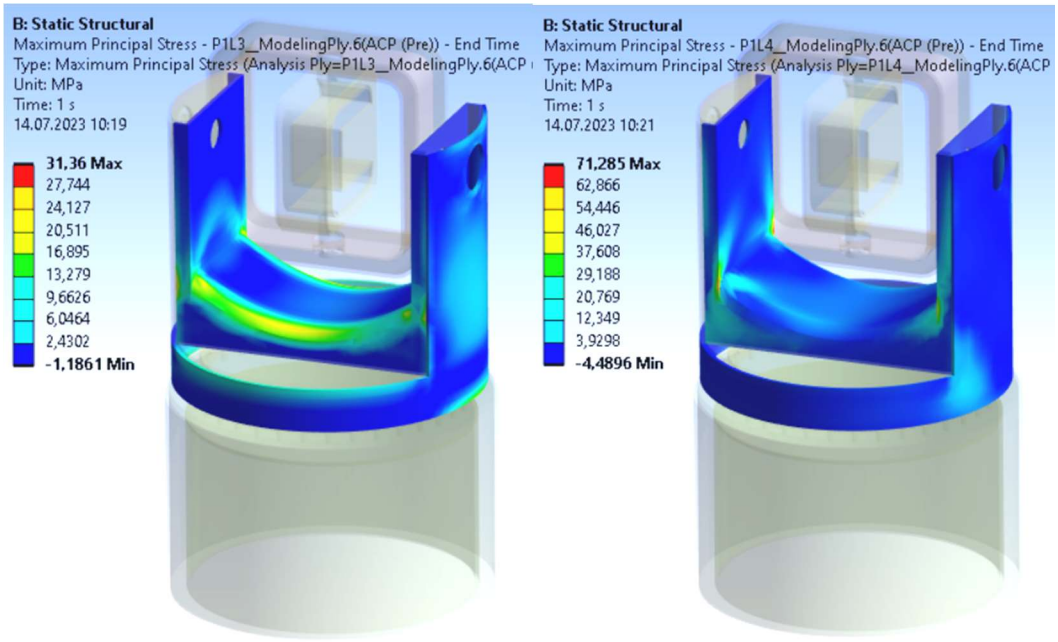

Figure 10. Stresses in the third and fourth layers of the composite

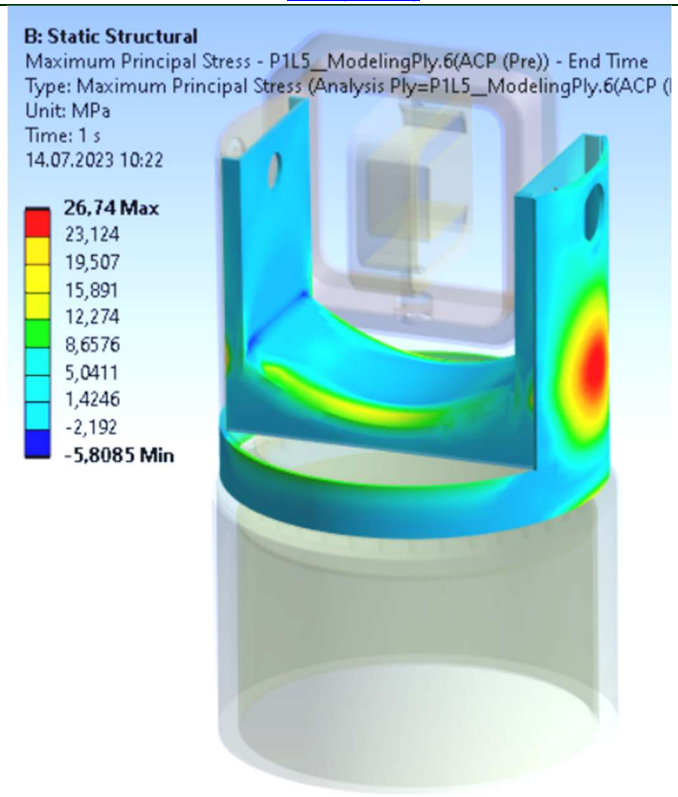

Figure 11. Stresses in the fifth layer of the composite

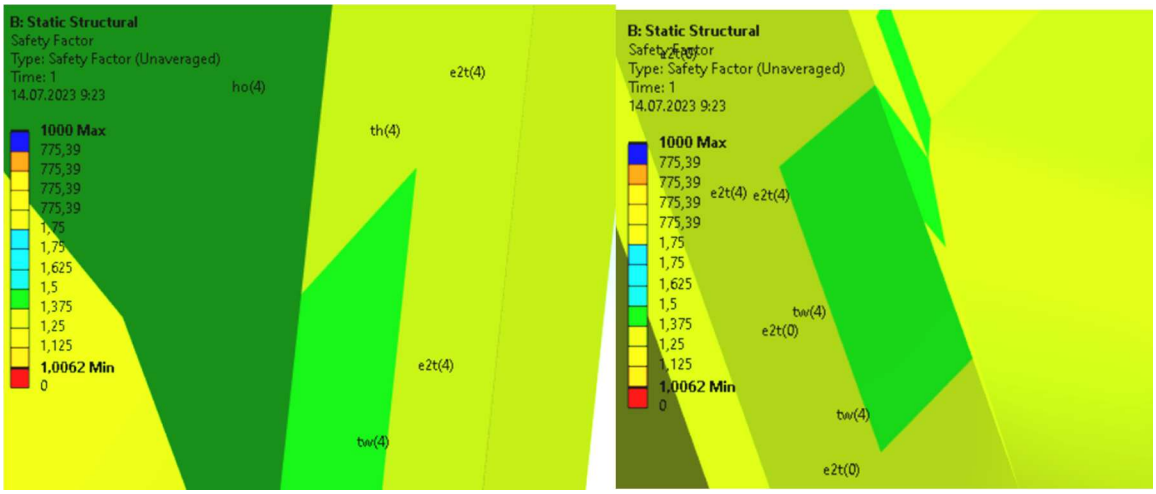

Figure 12. Maximum stresses in a five-layer package: e - deformation, 2 - direction, t - tension, the number in brackets means the number of the layer, tw - means the destruction of the layered structure ac-cording to the failure criterion of Tsai-Wu, th – Tsai-Hill, ho – Hoffman

Table 1. Physical and mechanical characteristics of magnesium alloy

Modulus of elasticity (shear), MPa	Poisson's ratio	Density, kg/m^3	Tensile strength, compression, MPa	Plastic limit in tension, compression, MPa
4,5×10^4(1.6×10^4)	0.35	1740	250	190

Table 2. Physical and mechanical characteristics of carbon fiber

Modulus of elasticity, MPa	Poisson's ratio	Shear modulus, MPa	Tensile strength, MPa	Ultimate compressive strength, MPa	Bending strength, MPa	Density, kg/m^3
0.85×10^5	0.27	0.82×10^4	395	240	470	1518

Table 3. Physical and mechanical characteristics of structural steel

Modulus of elasticity, MPa	Poisson's ratio	Shear Modulus, MPa	Tensile strength, MPa	Ultimate Compressive strength, MPa
2.0×10^5	0.3	76923	395	240

Table 4. Physical and mechanical characteristics of SAN Foam

Modulus of elasticity, MPa	Poisson's ratio	Shear Modulus, MPa	Tensile strength, MPa	Shear sz, MPa	Shear θz, MPa	Density, kg/m^3
60	0.3	23	1.1	0.8	0.8	81